© AUG 2025 | IRE Journals | Volume 9 Issue 2 | ISSN: 2456-8880
DOI: https://doi.org/10.64388/IREV9I2-1710213

Design And Fabrication of An Arduino Controlled Continuous Type Ginger Peeling Machine.

OKPARUBA, NOBLE C.[1], EZEANYA, NNAEMEKA C. [2], CHIKWUE, MAXWELL I [3], ASONYE, GLADYS U [4], IHEDIOHA, TOCHUKWU A.[5], UKOHA, COLLINS U.[6]

[1,2,3,4,5,6]*Department of Agricultural and Biosystems Engineering, Federal University of Technology Owerri (FUTO), Nigeria*

Abstract- Manual ginger peeling in Nigeria presents several challenges, including high labor demands, inconsistent peeling quality, increased processing time, and product loss. To address these inefficiencies, this research presents the design and fabrication of an automated ginger peeling machine integrated with an Arduino-based control system and a motorized conveyor. The system automates the entire peeling process from feeding to discharge, minimizing human involvement and improving productivity. The peeling mechanism employs abrasive rollers to gently remove the outer skin of ginger rhizomes, while the conveyor ensures continuous and uniform material flow. The Arduino microcontroller regulates motor speeds, conveyor timing, and system safety features, enabling precise and energy-efficient operation. Initial testing shows a substantial improvement in processing speed, consistency, and reduced operator fatigue. This innovation offers a scalable solution for small to medium-scale agro-processors, promoting mechanization in Nigeria's ginger value chain and contributing to enhanced product quality and export potential. In this research, to overcome the drudgery associated with the manual peeling method, and batch feeding process peeling an automatic and continuous type ginger peeling machine was designed, fabricated, and developed using Arduino programming as the control system with the aim of increasing the rate of peeling and to produce more evenly peeled ginger before further processing. A preliminary testing on the machine showed that the machine had a peeling time of 0.63 minutes, Peeling capacity of 104.08kg/hr and peeling efficiency of 92% respectively. The machine will aim to improve the post-harvest quantity and quality of peeled ginger, and also encourage production of ginger rhizomes in the country. By integrating smart technologies, the research aims to offer practical solutions with far-reaching impacts on the agricultural industry, economy, and environment.

Index Terms- Ginger Peeling Machine, Arduino microcontroller, Automation, Automated ginger peeling machine, motorized conveyor.

I. INTRODUCTION

The world is rapidly advancing toward the automation of virtually every human activity, driven by the integration of modern technology into industrial, agricultural, and domestic operations. As digital solutions become more accessible and affordable, individuals and organizations alike are increasingly adopting efficient, automated systems to improve productivity, reduce manual labor, and enhance accuracy. This shift reflects a growing reliance on intelligent machines and control systems to handle repetitive or labor-intensive tasks with minimal human intervention. In response to this global trend, the development of automated agricultural equipment—such as ginger peeling machines—has gained momentum, particularly in countries like Nigeria where agro-processing plays a significant role in the economy. Incorporating automation not only improves the quality and speed of processing but also aligns with global best practices in food handling, hygiene, and export competitiveness.

Peeling is a crucial post-harvest operation in ginger processing, essential for enhancing drying rates and preservation. Due to its irregular shape and delicate skin, mechanizing ginger peeling is challenging, leading to an inclination toward labor- intensive and time-consuming traditional methods that often result in significant product loss (Arocha & Simonyan, 2019). Lalthantluangi (2022) emphasized that manualI. ginger peeling methods are labor-intensive, time-consuming, and prone to inconsistencies and contamination risks. Mechanical peeling machines have emerged as effective alternatives, revolutionizing ginger processing with improved efficiency, consistency, and reduced labor needs. Even with mechanization, the predominant peeling machines utilized by Nigerian farmers are typically operated in batches, which introduces several inefficiencies into the processing operation. Batch processing often results in significant idle time between batches, leading to underutilization of equipment and increased energy consumption (Shinde et al., 2018).

Moreover, batch processing requires large spaces for staging, loading, and unloading of materials, which further exacerbates inefficiencies and limits overall productivity.

In contrast to batch processing, continuous systems operate without interruption, facilitated by conveyors that automate material handling, minimize errors, and ensure consistent processing conditions. These systems enhance efficiency, productivity, and adaptability in agro-processing (Malhotra, 2024). Integrating conveyors into continuous-type systems streamlines automation and sensing in processing machines (Ugoamadi, 2012). Van Colenberghe (2023) underscored that conveyors establish a structured pathway for material flow, enabling seamless integration of sensors along the line to monitor parameters like material presence and quality. Capacitive proximity sensors, for instance, detect material presence, triggering automated actions such as feeding or diverting. Additionally, conveyors provide a platform for incorporating automation technologies such as robotic arms for sorting and packaging. Centralized control systems and programmable logic controllers (PLCs) synchronize conveyor operation and equipment, facilitating real-time monitoring and adjustments (Ugoamadi, 2012). Academic research confirms the efficacy of this integration, showcasing enhanced efficiency and productivity. Overall, integrating conveyors into continuous-type systems optimizes processing, promoting competitiveness and sustainability in agro-processing (Malhotra, 2024).

II. LITERATURE REVIEW

Ginger rhizomes pose challenges for mechanical handling due to their irregular shape, particularly when only a thin skin layer needs removal. Attempts to use machines with abrasive rollers resulted in limited success, as prolonged abrasive peeling led to increased skin and tissue loss, reducing oil content recovery (Arocha & Simonyan, 2019). Kumar et al. (2019) developed a mechanical brush-type ginger peeling machine consisting of two continuous brush belts driven in opposite directions by a variable-speed motor. Peeling involves applying brushing force with opposed shearing elements, achieved through the movement of abrasive rollers and counter shear impact, relying on the material's inertia for shearing force.

Mechanical peeling is the use of knives or abrasive tools to remove the skin of fruits and vegetables (Gavahian & Sastry, 2020). Mechanical peeling is more suitable for fruits and vegetables that are regular in shape and have a hard texture, such as potatoes, carrots, apple, orange, kiwifruit, and several vegetables. For example, the most common method used in ginger rhizome peeling is mechanical peeling, but mechanical peeling results in about 25% peeling loss due to the irregular shape of ginger rhizome and leads to serious damage of essential oil cells (Kate & Sutar, 2018).

Lye peeling removes outer peel by synergistic effect of high temperature and chemical reaction, which is preferred in fruits and vegetables industry due to its higher effectiveness, wider application and better product quality (Lavelli, Pompei, & Casadei, 2009).
However, the wastewater with high chemical oxygen demand and pH causes environmental pollution problem and may have a negative impact on public health and food safety (Gao et al., 2018).

Hot-water peeling and steam peeling are considered as the best alternative method to lye peeling because of their environmental safety, but they generally result in mushy flesh, reduced firmness, and high peel loss (Vidyarthi et al., 2019; Vidyarthi, Li, & Pan, 2019). Besides, lye and hot-water peeling both involve intensive water consumption and generate a large amount of wastewater (Shen, 2020).

The process involves a gradual removal of material from a work piece additionally incorporating high-pressure equipment. Common abrasive processes are grinding,honing, sanding, polishing, buffing, lapping, abrasive water jetting, sand blasting and glass blasting.

Arocha & Simonyan (2019) designed and developed a motorized ginger rhizomes peeling machine with a capacity of 5 kilograms. The machine operates on the quadric-crank mechanism principle, converting rotary motion to oscillatory motion. Peeling is achieved through attrition or shearing force, facilitated by friction between the ginger and abrasive surfaces. A batch-type ginger washing and peeling machine was developed and tested for its effectiveness in the production of bleached dry ginger by Prasanna (2019). The machine utilized two hard nylon brush rollers rotating in opposite directions at 200 rpm to lift and tumble the ginger rhizomes while water jets removed soil and peels.

III. MATERIALS AND METHODS

According to Michael Ashby (2024), the varied requirements demanded of the materials are thus reduced to three broad demands and the include Fabrication requirements, Service requirements, and Economic requirement.

Despite significant advancements in ginger peeling technology, several critical gaps remain in the research and practical implementation of efficient peeling methods, particularly for the Nigerian context. There is a notable lack of research focused on continuous-type, Arduino controled ginger peeling systems that integrate automation technologies such as conveyor systems and capacitive proximity sensors (Ugoamadi, 2012; Malhotra, 2024). Such systems have the potential to enhance efficiency, reduce labor requirements, and provide consistent processing conditions, thus addressing the limitations of batch processing (Malhotra, 2024).

Therefore, there is a clear research gap in developing a smart, continuous-type, Arduino control ginger peeling machine tailored to the needs of Nigerian farmers.

3.1 DESIGN CONSIDERATIONS.

The basic design considered or employed in the design and fabrication of a smart and continuous ginger peeling machine is that of Survey to examine the conditions abrasive materials on the peeling effects or action on ginger tuber considering the irregular shape of ginger tubers, and to find the best type of abrasive material, the best speed and force required to effect the peeling/removal of the outer coating of shells of ginger to tubers. In order to obtain high efficiency and capability, the machine was designed based on the following consideration:

i. It was fabricated from locally sourced materials and within the purchasing capacity of local farmers and processors.
ii. It was fabricated to peel different varieties, shapes and sizes of ginger and have reasonable peeling efficiency.
iii. It was able to work continuously with little to no human supervision.
iv. High in capacity compared to manual and hand peeling operations/methods
v. Ability to reduce the labour intensive and drudgery associated with traditional method of ginger peeling.

Also considered was the decision having to do with material selection and their properties together with other design factors were also carefully considered in this project.

Some of the design factors considered are as follows: Factor of Safety, Maintainability and Serviceability, Durability and portability, Corrosion resistance, Effect of friction, Availability, Stability during operation

© AUG 2025 | IRE Journals | Volume 9 Issue 2 | ISSN: 2456-8880
DOI: https://doi.org/10.64388/IREV9I2-1710213

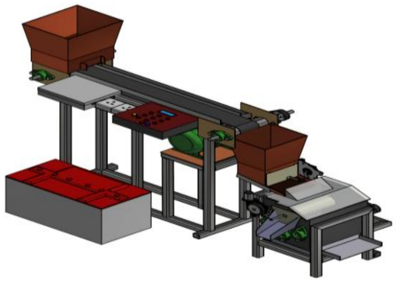

Figure 1: Isometric View of the Ginger Peeling Machine

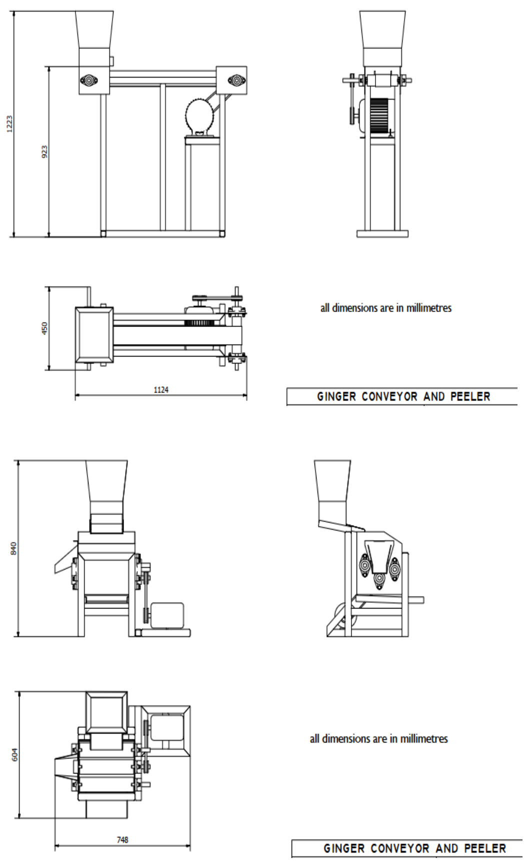

Figure 2: Orthographic Views of Machine; Conveyor Part (Top) and Peeler Part(Bottom).

3.2 Machine Design and Fabrication

The machine was designed based on a conceptual design that was drawn with AutoDesk Inventor CAD (V.2021b) software application as shown in Figures 3.1 to 3.6. The drawing employed the frame generator, part drawing of each component with careful detailing. The part drawings was followed by a careful assemble drawing where all components were carefully merged using appropriate methods expected to be actualized and constrained based on the expected operation movement or rigidity of these components. Each component thus has different degree of freedom (DoF).

The fully assembled machine was thereafter presented in various appropriate views with accurate measurement to aid correct development as shown in Figures 2.

The machine was developed with careful consideration of the materials employed, component specifications, research site, available fabrication equipment, and cost reduction strategies. Fabrication took place at the Federal University of Technology Owerri workshop 2, utilizing techniques including welding, machining, sheet metal processing, assembly, and temporary attachment.

Electrical connections were made using suitable methods and guidelines for the PV system, electric motor, and control unit. The machine's components were fabricated and dimension in accordance with the designs depicted in Figures 1. The ideal dimensions for various machine parts were determined through diverse design calculations.

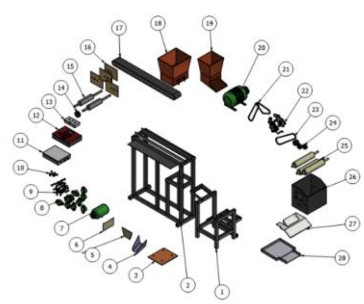

ITEM NO	ITEM DESCRIPTION	QTY
1	Peeling Machine Frame	1
2	Conveyor Frame	1
3	Conveyor Engine Base Plate	1
4	Ginger Discharge Chute	1
5	Discharge Chute Cover	1
6	Infeed Gate Cover	1
7	Peeling Machine Engine	1
8	Flat Bearing	10
9	Bolts	24
10	Nuts	24
11	Speed Control Box	1
12	Arduino Microcontroller Box	1
13	Control box Sockets	2
14	Conveyor Roller Pulley	1
15	Conveyor Roller	2
16	Conveyor Side Plate	4
17	Conveyor Belt	1
18	Conveyor Hopper	1
19	Peeling Machine Hopper	1
20	Conveyor Engine	1
21	Peeling Machine V-belts	2
22	Inlet and Outlet Motor	2
23	Conveyor Engine V-belt	1
24	Peeling Engine Pulley	3
25	Peeling Cylinder	2
26	Ginger Peeling Chamber	1
27	Peeling Chamber Cover	1
28	Trash Tray	

Figure 3: Exploded View of the Machine

3.3 Design Calculations

The ginger to be peeled and the various components of the ginger peeling machine would be subjected to varying forms and degrees of stress, strain, torque, and vibrational effects. The materials with the appropriate engineering properties were chosen based on the design calculations.

3.4 Detailed Analysis of Components:

The detailed analysis of the various parts and components of the peeling machine which makes up the full assembly and thus analyzed as follows:

3.4.1 Hopper Design

In designing the hopper, the angle of inclination of the hopper walls was set to be 10 degrees higher than the natural angle of repose of ginger rhizome to prevent tunneling and arching during discharge. The hopper shape resembled a frustum of a pyramid. Given that the angle of repose for ginger ranges from 41.3° to 51.6° (Ajav & Ogunlade, 2014), an angle of inclination of 62° was utilized in the hopper design. The volume of the hopper was determined using the equation provided by Ugoamad. (2012).

3.4.2 Volume of Conveyor System Hopper

The conveyor system hopper was designed to have the regular shape of a truncated pyramid for easy construction/fabrication and also to enable the ginger tubers to flow through the discharge end freely into the conveyor belt.

A truncated pyramid that is chopped of from the tip with a plane parallel to its base. This is shown in the Figure 4.

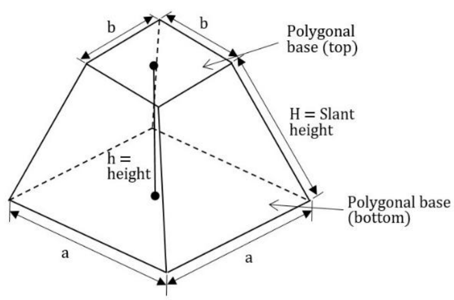

Figure 4: A Truncated Pyramid of a Hopper.

The volume of the truncated pyramid which is the hopper shape can be calculated with the standard formula of a frustum of a pyramid.

$$V = \frac{1}{3} h \left(a^2 + \ b^2 \ ab\right) \qquad (1)$$

Where
a = lower base length
b = upper base length
h = vertical height
But for the case of our designed conveyor hopper is a regular truncated rectangular pyramid pond which has the following designed dimensions as shown in Figure 5.

The standard formula applied or used is as follows;

$$\text{Volume } V = \frac{Ab+ab+2\ (ab+Ab)}{6} \times \ h \qquad (2)$$

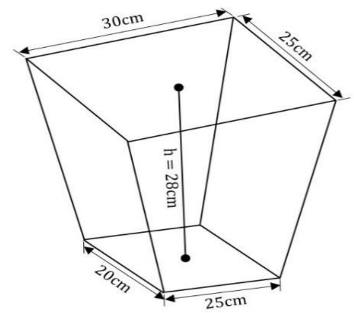

Figure 5: A Conveyor system Hopper with Dimensions.

Were
A = 30cm, B = 25cm, a = 25cm, b = 20cm, h = 28cm
Hence applying the formula above, we have the volume calculated as,

$$V = \frac{Ab+ab+2\ (ab+Ab)}{6} \times \ h$$

$$V = \frac{30\times20+25\times25+2\ (25\times20+30\times25)}{6} \times \ 28$$

$$V = \frac{600+625+2(500\times750)}{6} \ \times 28$$

$$V = \frac{600+625+2500}{6} \ \times 28 \quad = \frac{3725}{6} \ \times 28$$

$$V = 620.83 \times 28$$

Volume of Hopper, V = 17,383.3cm^3

3.4.3 Volume of the Peeling Chambers

The volume of the peeling chambers which has the designed shape of a regular rectangle can be calculated or determined using the standard formula of a regular rectangle as shown below.

The peeling chambers has the following designed dimensions as shown also in figure Fig 3.12.

© AUG 2025 | IRE Journals | Volume 9 Issue 2 | ISSN: 2456-8880
DOI: https://doi.org/10.64388/IREV9I2-1710213

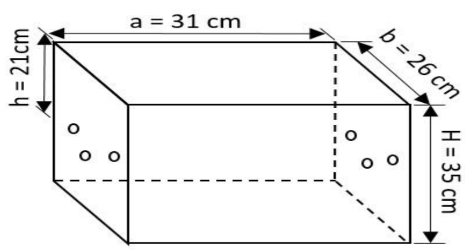

Figure 6: Ginger Peeling Chambers

Where:
Length, a = 31cm, Width, b = 26cm, Total height, H = 35cm, Active height, h = 21cm
From the standard formula for volume of a regular rectangle, it is the product of the length, width, and height; that is, Length x Width x Height.
Hence the volume of the ginger peeling machine can be calculated in two forms or categories;

- The Total Volume of The Peeling Chambers.
  The total volume of the peeling chambers is calculated as follows.
  Volume of rectangle, $V = L \times W \times h$ (3)
  That is, $V = 31 \times 26 \times 35 = 28{,}210$
  Total Volume, V= 28,210 cm^3
- Effective or Active Volume of Peeling Chambers.

The effective or active volume of the ginger peeling chambers is the actual volume or portion of the peeling chambers that is actually utilized in peeling the ginger tubers. This is the part above the three abrasive cylinders rotating along their axis effecting a peeling action on the tubers.

The dimensions are also as follows:
Length, L = 31cm
Width W = 26cm
Height h = 21cm
Hence Volume, $V = L \times W \times h$
$V = 31 \times 26 \times 21 = 16{,}926$
Effective Volume V = 16,926 cm^3

3.4.4 Motor Design Selection - Peeling Chamber

The drive motor designed and selected for the ginger peeling machine is an AC. powered Electric motor which has the following rating or parameters. The ginger peeling machine peeling chamber is where the peeling or removal of the outer skin (shell) of ginger tubers are carried out.

AC Motor Rating:

Voltage VAC	=	220V
Amperage A.C (Current IA)	=	2.3A
Resistance Ra	=	0.01Ω
Speed (Revolution) Vm rpm.	=	1500
Shaft diameter, Da (15mm)	=	1.5cm
Phase	=	1
Power factor Pf	=	0.8

Power delivered by the AC. motor, is Pm.

And Power $P_A = IV$ = Apparent power (4)
Were. I = 2.3
V = 220
$P_f = 0.8$

Hence, Apparent = IV = 2.3 x 220 = 506V A
Thus, Active Power, $P_m = VA \times P_m = 506 \times 0.8$
Or Active Power = 2.3 x 220 x 0.8 = 404.8 Watts

i.e., Active power delivered by the drive motor to the shaft is Pm = 404.8 Watts
P_m = 404.8 Watts = 0.405 kw.

This is the active power transmitted from the AC motor to the shafts of the peeling shafts in the peeling chamber.

The torque transmitted by the drive motor shaft to the peeling shafts and cylinders. is represented by T_m.
And T_m is given by, $\frac{60 \text{ x Power}}{2\pi \text{ x RPM}}$

Torque, T_m is the product of the force acting or the body and the perpendicular distance given point to the line of action of the equivalent to a couple acting upon a body.

From the power, Speed and torque relation we have that power of the motor P_m is given by

$$P_m \text{ (KW)} = \frac{2\pi \text{ x speed (rpm) x torque}}{60} \quad (5)$$

Thus, $\text{Torque (KNm)} = \frac{60 \text{ x Power (Kw)}}{2\pi \text{ x Speed (rpm)}}$

Hence, $\text{Torque (Nm)} = \frac{9548.\text{X Power (KW)}}{\text{Speed (rpm)}}$

© AUG 2025 | IRE Journals | Volume 9 Issue 2 | ISSN: 2456-8880
DOI: https://doi.org/10.64388/IREV9I2-1710213

Were,
Power, P_m (kW) = 0.405 Kw
Speed (rpm) = 1500 rpm
Constant factor = 19548 $\quad 60\left(\frac{1000}{2\pi}\right)$

Therefore, Torque $T_m = \frac{9548 \text{ x } 0.405}{1500} = 2.57796$

Torque T_m = 2.58 Nm.

This is the torque transmitted by the motor shaft to the peeling shaft and peeling Cylinder.

3.4.5 Torque on Peeling Shaft.

The rotational count counterpart of force in physic is torque and is always represented by T. Torque is a crucial component of virtually every kind of engineering application, every machine that has a rotating Shaft includes torque Component, which accounts for almost the entire transportation world, agriculture and equipment, industrial machines etc.

From force, torque and speed relation, the torque formula can be written as,
T = F x r x sin Ө

Where:
F = is the force applied to the lever or rotating shaft of length, r at an angle Ө, since sin 0^0 = 0 and sin 90=1, we see that torque is maximized when the force is applied perpendicular to the lever or shaft.
For all shaft torque, we must specify the kind of shaft concerned because solid and hollow shafts behave differently when subjected to force and torque on the same diameter. But the motion power in (kw) is 0.405 kw, and the motor torque is 2.58 Nm.

The motor shaft torque can be calculated from these expressions,

Output in Watts $= \frac{2\pi N}{60} T_{sh}$ Watt (6)

Where, T_{sh} is the torque on the motors shaft

$T_{sh} = \frac{\text{Output in watts}}{2\pi N}$ Nm in rps

$T_{sh} = \frac{\text{Output in watts}}{\frac{2\pi N}{60}}$ Nm in rpm

$T_{sh} = \frac{\text{motor output}}{\frac{2\pi N}{60}}$

Hence,

$T_{sh} = \frac{60}{2\pi} \text{ x } \frac{\text{output}}{N} = 9.55\,\frac{\text{output}}{N} = \left(\frac{60}{2\pi} = 9.55\right)$

Where, N = 1500

Therefore, motor shaft Torque, Tsh = $9.55\,\frac{404.8}{1500}$

$\frac{9.55 \text{ x } 404.8}{1500} = \frac{3865.84}{1500} = 2.577$

T_{sh} =2.580 Nm

This shows that there is no loss on the torque transmitted from the motor armature to the motor shaft.

3.4.6 Shaft Design

In this research, we selected a shaft made of mild steel or low carbon steel material. Transmission shafts are designed on the basis of strength, rigidity and stiffness. For this project work, the power transmission shaft is designed based on the strength of the material and which is a shaft that is subjected to combined twisting and bending moments. It is therefore designed on the basis of the two moments simultaneously.

Applying the maximum shear stress theory or the guest's theory which is used for ductile materials such as the mild steel or low carbon steel and maximum normal theory or Rankine theory

Let,
τ = shear stress induced due to twisting moment and
σ_b = Bending stress (Tensile and Compressive) induced due to bending moment.
According to maximum shear stress theory, the maximum shear stress acting on the shaft is

$$\tau_{max} = ½\sqrt{(\sigma_b)^2 + 4\tau^2} \quad (7)$$

Substituting the values of τ and σ from a Shaft subjected to both twisting and bending moments only, we have that,

$$\tau_{max} = ½\sqrt{\left(\frac{32}{\pi d^3}\right)^2 + 4\left(\frac{16T}{\pi d^3}\right)^2} = \frac{16T}{\pi d^3}\left[\sqrt{M^2 + T^2}\right]$$

3.11

Or $\frac{\pi}{16}$ x τ_{max} x $d^3 = \sqrt{M^2 + T^2}$

© AUG 2025 | IRE Journals | Volume 9 Issue 2 | ISSN: 2456-8880
DOI: https://doi.org/10.64388/IREV9I2-1710213

This is known as the equivalent twisting moment denoted by, T_e which when acting alone produces same stress (τ) as the actual twisting moment. By limiting the maximum shear stress (τ_{max}) equal to the allowable shear stress (τ) for the material, equation 3.11 above may be written on as

$$T_e = \sqrt{M^2 + T^2} = \frac{\pi}{16} \text{ x } \tau \text{ x } d^3 \quad (8)$$

According to maximum normal stress theory, the normal stress in the shaft is given as,

$$= ½\, \partial_b + ½ \sqrt{(\partial_b)^2 + 4\tau^2} \quad (9)$$

$$= ½ \frac{32M}{\pi d^3} + ½ \sqrt{(\frac{32M}{\pi d^3})^2 + 4(\frac{16T}{\pi d^3})^2} \quad (10)$$

$$\frac{32M}{\pi d^3} [½ (M + \sqrt{M^2 + T^2}\ ] \quad (11)$$

$$\frac{\pi}{32} \text{ x } \partial_b \text{ x } d^3 = ½ [M + \sqrt{M^2 + T^2}\ ] \quad (12)$$

This expression (12) is the equivalent bending moment denoted by M_e which when acting alone produces the same tensile or compressive stress (J_b) as the actual bending moment. By limiting the maximum normal stress ($J_{b(max)}$) equal to the allowable bending Stress (J_b), the equation (12) may be written as

$$M_e = ½ (M + \sqrt{M^2 + T^2} = \frac{\pi}{32} \text{ x } \partial_b \text{ x } d^3 \quad (13)$$

In case of a hollow shaft, the equations (8) and (12) may be written as,

$$T_e = \sqrt{M^2 + T^2} = \frac{\pi}{16} \text{ x } \tau\, (do)^3\, (1-K^4) \quad (14)$$

$$Me = ½ (M+ \sqrt{M^2 + T^2} = \frac{\pi}{32} \text{ x } \partial_b (do)^3\, (1-K^4) (15)$$

Where, K= ratio of inside and outside diameter at the shaft = d_i/d_o (Khurmi & Gupta, 2014).

But in this research a solid shaft was used for the transmission of power and motion, hence equations (8), (9) and (12) were used to determine the diameter of the shaft to be used in the project. This suggests that diameter of the shaft may be obtained or determined by using both the theory and the larger of the values ie two values are obtained.

3.4.7 Belt and Pulley Design.

A V-belt and pulley system was selected for the design for power transmission because of its advantages for the reduced tendency of slippage and the relatively short distance of travel.

The choice and selection of a V-belt for the transmission of rotary motion power from the A.C 220V drive motor to the drive shafts of the peeling cylinders or drums was based on obtaining a trouble free system and longer life of the machine. The V-belt selected is made of fabric cord usually cotten materials, impregnated with rubber for improved strength and resistance to wear and tear. The V-belt selected as shown in Figure 7 has the following dimensions and characteristics.

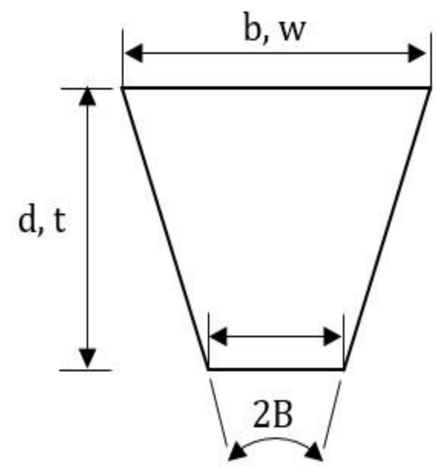

Figure 7: V-Belt Showing Dimensions

DRIVEN DRIVER
(i) w, b = Groove width
18mm 16mm
(ii) d, t = Groove depth or thickness =
13 mm 11 mm
(iii) 2β = groove angle in degrees = 32^0
(iv) n = Number of sheave groove = 6mm

The pulley selected for both the driver and the driven belongs to the "A" type of pulleys and belts for the design.

© AUG 2025 | IRE Journals | Volume 9 Issue 2 | ISSN: 2456-8880
DOI: https://doi.org/10.64388/IREV9I2-1710213

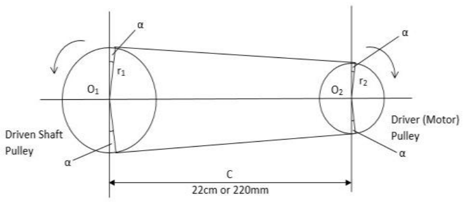

Figure 8: A Driver Pulley and Driven Pulley with Belt of an Open Belt Dive.

The driver Speed, N_1 = 1500 rpm

The driven speed, N_2= 1333 rpm= $(\frac{16}{18} * 1500)$=1333

The face or groove width (b) of the driver pulley is equal to = 16mm.

The face or groove width of the driven (shaft) pulley is equal to = 18mm

The torque on the driver pulley attached to the electric motor of power 404.8 Watts = 0. 405 KW.

Power, P_m = 404.8 Watts

$N = \frac{1500}{60} = 25$ rev/sec.

$$\text{Torque} = \frac{\text{Power}}{2\pi N} \quad (16)$$

$$\frac{404.8}{2 \times \pi \times 25} = 2.576$$

Torque T_m = 2.58 Nm.

For the driven pulley attached to the shaft of the peeling cylinder,

Power transmitted, P_m = 404.8 Watts.

$N = \frac{1333}{60} = 22.2$ rev/sec.

$$\text{Torque Tsh} = \frac{\text{Power}}{2\pi N} = \frac{404.8}{2 \times \pi \times 22.2} = \frac{404.8}{139.486} = 2.902$$

Torque T_{sh} =2.90Nm

The dimensions of the two pulleys are:

Driver pulley, D_1 = 7cm (70mm) or r_1 =3.5 cm (35mm)

Driven pulley, D_2 = 5.7cm (57mm) or r_2 = 2.85cm (28.5mm)

Distance between pulleys, C = 22cm (220mm)

Hence, the belt length, L is determined using the expression

$$L = \pi (r_2 + r_1) + 2c + \frac{(r2 - r1)2}{C} \quad (17)$$

$$= \pi (D_2 + D_1) + 2c + \frac{(D2 - D1)2}{4C} \quad (18)$$

Thus, working with the radius of the two pulleys, we have the length of the belt (Pitch length of the belt), L as:

$$L = \pi (r_2 + r_1) + 2c + \frac{(r2 - r1)2}{C} \quad (19)$$

$$= \pi (35 + 28.5) + 2 \times 220 + \frac{(35 - 28.5)2}{220}$$

= 192.52 + 440 + 0.192 = 639.71

L = 639.71mm or 0.639 m.

The contact angle between the belt and pulley is Θ_t = sin $\propto$

And $\Theta_t = \sin_{-1} \frac{(D2 - D1)}{2C}$

$= \sin^{-1} \frac{(70 - 57)}{2 \times 220} = \frac{13.0}{440} = 0.02954$

i.e $\sin^{-1}$ 02954 = 1.6927 1.69^0

$\Theta_t = \sin^{-1} \alpha = 1.69^0$

From the Diagram Figure 9 it shows the production drawing of pully showing all dimensions.

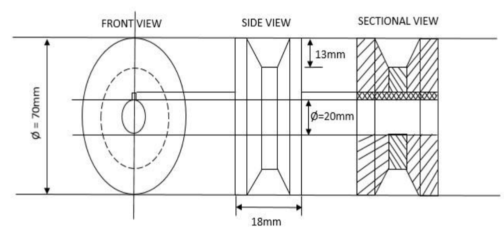

Figure 9: Production drawing of Pulley Showing dimensions.

3.4.8 Conveyor Belt Design

The conveyor belt is an essential equipment in large scale manufacturing and processing industries and its technology is straight forward. An electric motors powers the system driving one or more pulleys attached to one or more shafts that drives the belts along in a continuous flow. The belt rest on a plate bed or rollers for their easy and continuous flow.

The entire Conveyor belt system Comprises of the following parts.

(1) The belt: It is the most obvious part of the system.
(2) Motor: Provides the energy and power to drive the entire system.

© AUG 2025 | IRE Journals | Volume 9 Issue 2 | ISSN: 2456-8880
DOI: https://doi.org/10.64388/IREV9I2-1710213

(3) Pulleys: Assists the motor to transfer the rotary motion into linear motion to drive the system.
(4) Roller: Provider support to the belt and good surface for the belt to move freely
(5) Bearing: Provides guide support to the rollers and shafts for easy movement of the belt.
(6) Frame: Provide support and guideways to the belt and other parts of the Conveyor system.

To ensure safe and efficient conveyor system or efficient conveying of goods and materials from one point to another, it is essential to consider the following design factors namely size, shape, weight, fragility, and orientation of the material or product being transported.

The conveyor belt for this project was considered based on the low cost and the availability of the belt material. A polyester material is thus selected for the design of the conveyor belt.

3.4.9 Conveyor Belt Length.

The designed conveyor belt system is a horizontally mounted belt conveyor system as shown in figure 10. The length of the belt was calculated according to khumi and Gupta (2014) and expressed in equation (20).

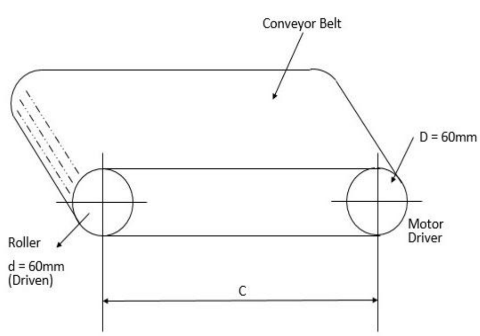

Figure 10: Conveyor Belt Showing Dimensions.

Where:
C = 960mm = Center to Center distance
D = 60.0 mm = Diameter of driver pulley or roller
d = 60.0mm = Diameter of driven pulley as roller
π = 3.142 Pi (a Constant).

Hence the formula for the length is

$$L = \left(\frac{D + d}{2} \times \pi\right) + 2c \qquad (20)$$

$$\left(\frac{60.0 + 60.0}{2} \times \pi\right) + 2 \times 960 = 188.5 + 1920 = 2108.5$$

Length, L of the belt. = 2108.5 mm = 2.11m

3.4.10 Material Load on the Conveyor Belt.

This is the total weight of the material on the conveyor belt which is uniformly loaded or distributed on the belt as it conveys them from the infeed conveyor hopper to the next point. In this case. The total load of the materials on the conveyor belt represented by F_{total} can be calculated using the formula

$F_{total} = (m + m_b \times L) \times g$

Were,
M = mass of load on the belt in Kg
M_b = mass of belt itself in kg
L = length of the belt
G = gravitational force (9.81)

From our previous calculation and result obtained, we have that
M = 36.0 kg (weighted)
M_b = 0.5 kg (weighted)
L = 2.11 m
G = 9.81 (Constant given)

Applying the formula for total material load F_{total}
F_{total} = (36.0 + 0.50 x 2.11) x 9.81
= 77.02 x 9.81 = 755.517
F_{total} = 755.52N

3.2.6.11 Conveyor Belt Speed.

Conveyor belt speed is the speed at which the conveyor belt moves typically measured in meters per minute ($Mmin^{-1}$) or feet per minute ($fmin^{-1}$). The belt speed influences the capacity of the conveyor. Higher speeds increase throughput but may also require more power and a stronger belt material. The conveyor belt speed was determined by using the formula

Speed, $V = \frac{\pi \times D \times rpm}{60}$ measured in ms^{-1}

$$\text{That is } V = \frac{\pi \times D \times rpm}{60} \qquad (21)$$

Where π = dimensionless constant = 3.142
D = diameter of the drive rollers = 0.06m
RPM = motor speed in rpm = 2800rpm

© AUG 2025 | IRE Journals | Volume 9 Issue 2 | ISSN: 2456-8880
DOI: https://doi.org/10.64388/IREV9I2-1710213

Therefore, $V = \frac{3.142 \times 0.006 \times 1500}{60} = \frac{282.8}{60}$

$V = 4.71 \quad = 4.7m/s$

Belt conveyor speed, V = 4.7m/s

3.4.12 Conveyor Power Requirements.

This is the power requirements to drive or cause the conveyor system belt to move the material from the in-feed conveyor hopper to the next point on the process line. (Peeling chamber) is known as a power required donated by P. The following formula is used to calculate the power required

We have $P = \frac{(F \times V)}{\eta}$ (22)

Were,

F = Total load on the Belt (N) = 755.52N

V = Belt speed (m/s) = 8.80m/s

η = Drive efficiency (Dimensionless often a percentage) 95% = 0.95

P = Power required in kilowatt

Therefore, Power (KW) = $\frac{(755.52 \times 8.8)}{0.95} = \frac{6648.58}{0.95}$

Power, P = 6998.5KW.

3.4 Development of the automation system

3.5.1 Hardware Materials used in the Automation Unit

The following is a list of the hardware materials used in the automation unit of the machine along with a brief explanation of their roles:

i. Arduino Microcontroller:
The Arduino acted as the central control unit for the system. It processed input from the keypad, controlled the relays and motors, and displayed real-time feedback on the LCD.

ii. I2C LCD (20x4):
This LCD provided a user interface for displaying system prompts, timers, and status messages. The I2C interface reduced wiring complexity by using only two communication lines.

iii. 4x4 Keypad:
The keypad allowed users to input the desired timing durations for the conveyor and peeler. It also facilitated starting and resetting the system through specific key presses.

iv. Relays (2 Units):
Relays were used to switch the AC motors for the conveyor and peeler on and off. They acted as intermediaries between the low-power controls signals from the Arduino and the high-power AC circuits.

v. AC Motors:
a. Conveyor Motor: Powered the conveyor to move ginger from the inlet to the peeler.
b. Peeler Motor: Drove the peeling mechanism to process the ginger effectively.

vi. AC Motor Speed Controllers (with Knob):
These controllers regulated the speed of the AC motors. Each controller featured a knob (potentiometer) for manual adjustment, allowing fine-tuning of motor speeds to suit processing requirements.

vii. DC Motors (2 Units):
a. Inlet Door Motor: Opened and closed the inlet door for loading ginger.
b. Outlet Door Motor: Opened and closed the outlet door for discharging processed ginger.

viii. Motor Driver (L298 or Equivalent):
The motor driver enabled the Arduino to control the direction and activation of the DC motors. It provided the necessary power amplification and directional control signals.

ix. Power Supply:
A regulated power source supplied the required voltage and current to power the Arduino, LCD, relays, motor driver, and motors.

x. Potentiometer (Knob on Speed Controller):
This adjustable knob allowed users to manually set the speed of the AC motors for the conveyor and peeler, providing flexibility for different ginger processing needs.

xi. Wires and Connectors:
These were used to establish electrical connections between components, ensuring stable communication and power transmission.

xii. Base Structure:
A sturdy frame was used to securely mount the motors, conveyor, peeler, and other mechanical components, ensuring system stability during operation.

xiii. Resistors and Diodes:
a. Resistors: Used in pull-up or pull-down configurations in the keypad or motor driver circuits.

b. Diodes: Protected the system from back-emf generated by motors and relays, ensuring component safety.

3.6 The Principle of Operation of the System

The principle of operation of the microcontroller-based smart sequential automation system for ginger processing revolves around the integration of relays, direct current (DC) motors, a keypad, and an Inter-Integrated Circuit Liquid Crystal Display (I2C LCD) for the automation and control of tasks such as conveying, peeling, and opening or closing the inlet and outlet mechanisms. The system is designed to handle multiple stages of ginger processing efficiently by coordinating these components in a predefined sequence based on user-specified timing.

An Arduino microcontroller is at the heart of the system, and it serves as the central processing unit. The microcontroller is programmed to manage all operations based on input from a 4x4 matrix keypad and to display real-time feedback on a 20x4 I2C LCD screen. The user interacts with the system by entering the desired processing durations for the conveyor and the peeler using the keypad. These timings are input in seconds and are internally converted into milliseconds for precise time management. Once the inputs are provided, the system waits for the user to confirm the start of the operation by pressing the '#' key on the keypad.

The system begins by activating the conveyor mechanism, which is controlled via a relay. The relay acts as a switch to power the conveyor motor, enabling it to transport ginger from the inlet to the processing area. Simultaneously, the inlet mechanism, controlled by a DC motor, opens to allow the ginger to enter the conveyor system. The motor's rotation is controlled using two digital output pins connected to the Arduino, which drive the motor in forward or reverse directions, thereby opening or closing the inlet.

As the conveyor operates, the LCD provides a countdown of the remaining conveyor operation time, ensuring that the user is always informed about the system's progress. Once the conveyor operation is complete, the system halts the conveyor motor and closes the inlet door by reversing the motor's direction. This ensures that no additional ginger enters the system until the current batch has completed processing.

The system then transitions to the peeling stage. The peeler mechanism is activated using another relay, which powers the peeler motor. Simultaneously, the outlet mechanism, also controlled by a DC motor, remains closed to prevent processed ginger from exiting prematurely. The peeler motor operates for the duration specified by the user, and the remaining time is displayed on the LCD. Once the peeling operation is complete, the system deactivates the peeler motor and opens the outlet mechanism by driving the outlet motor in the forward direction. This allows the peeled ginger to exit the system. After a brief delay to ensure all processed ginger has exited, the outlet mechanism is closed by reversing the motor's direction.

Throughout the operation, the system employs a combination of non-blocking time management using the `millis()` function and a state-based control structure. This ensures that multiple processes can run concurrently without interference. For example, while the conveyor and inlet mechanisms are active, the system can simultaneously monitor the peeling operation and prepare the outlet mechanism for activation. The use of non-blocking code improves the system's responsiveness and reliability, particularly in scenarios where precise timing is critical.

The relays used in the system act as intermediary devices between the low-power Arduino outputs and the high-power motors. This allows the Arduino to control devices that operate at higher voltages or currents than the microcontroller can directly handle. The DC motors controlling the inlet and outlet mechanisms are driven in a bidirectional manner, enabling them to perform both opening and closing actions as required. This bidirectional control is achieved by setting the appropriate logic levels on the motor driver input pins.

To ensure safe operation, the system is initialized in a default state where all relays and motors are deactivated. This prevents unintended activation of any component during power-up or when no timings are specified. Additionally, the user is provided with a reset functionality that halts all operations and clears the LCD, preparing the system for the next batch of operations.

The I2C LCD plays a crucial role in providing real-time feedback to the user. It displays prompts for entering timings, ongoing process status, and completion messages. This visual feedback enhances the system's usability by ensuring the user is always aware of the current state of the operations. For instance, during the conveyor operation, the LCD displays the remaining time and indicates that the inlet is open. Similarly, during the peeling stage, it shows the countdown and confirms the outlet's status. The system is designed to handle the sequential automation of ginger processing tasks with minimal user intervention.

The operation of the conveyor and peeler in the system relied on AC motors, which were controlled using dedicated AC motor speed controllers. These speed controllers included a built-in knob (potentiometer) that allowed for manual adjustment of the motor speed. This feature was crucial for ensuring precise operation, as the speed of the motors could be varied to meet specific requirements for different stages of ginger processing. By adjusting the knob, the system maintained optimal performance for both the conveyor and the peeling mechanism, ensuring efficient and uniform processing.

The AC motor speed controllers were integrated into the system through relays, which acted as switches to control the motors' operation. The relays were activated by the Arduino microcontroller, which determined when to start and stop the motors based on user-defined timing inputs and the process sequence. Once a relay was activated, the speed of the motor could be fine-tuned using the speed controller's knob, ensuring smooth operation and consistent output.

This manual speed adjustment capability offered several advantages, including enhanced flexibility to handle varying ginger sizes and processing loads, reduced mechanical stress on the motors, and improved energy efficiency. The integration of the speed controllers and their adjustable knobs ensured that the system was adaptable, efficient, and capable of delivering high-quality processing results for ginger.

3.6.1 System Circuit Diagram

The circuit diagram of the system is shown in figure (10)

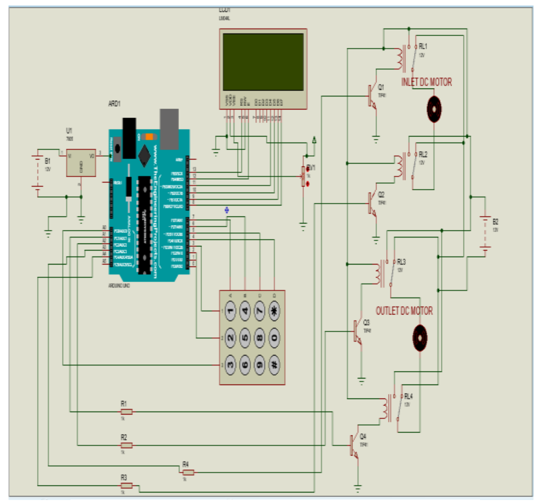

Figure 10: The System Circuit

3.7 Preliminary Testing.

Preliminary testing was conducted to evaluate machine peeling efficiency, time of peel and peeling capacity. Freshly harvested ginger rhizomes (variety: Nadia) were bought from Umuguma market .The power system was initiated, along with the electric motors of the conveyor and peeling machine. An Arduino controlled continuous type ginger peeling machine was designed and fabricated, the machine was tested and performance evaluation carried was out. The brush rollers operated at a specific rotary speed, and the conveyor functioned at a predetermined speed to maintain a consistent feeding rate.

IV. RESULTS

After building the device, both the Arduino program and all the circuit designed worked successfully. The controlled components and mechanical component parts worked synchronously. A preliminary testing on the machine showed that the machine had a peeling time of 0.63 minutes, Peeling capacity of 104.08kg/hr and peeling efficiency of 92% respectively.

CONCLUSION

The system successfully integrated multiple components to execute task sequentially, including the transport of ginger via the conveyor, the peeling process, and the controlled operation of the inlet and outlet doors.

The inclusion of an I2C LCD provided clear, real-time feedback to the user, displaying prompts, countdown timers, and task statuses. This feature enhanced user interaction and ensured that the system was easy to operate. The 4x4 keypad allowed users to input custom timing durations for each stage, making the system adaptable to different processing requirements.

The AC motor speed controllers with adjustable knobs played a pivotal role in achieving precise control over the conveyor and peeler motors. By manually setting the speeds, users could optimize the performance of the system for varying ginger sizes and quantities. The DC motors for the inlet and outlet doors, controlled by the motor driver, operated smoothly and accurately, facilitating efficient material flow through the system.

The relays and power supply ensured reliable operation of the high-power components, while the Arduino microcontroller managed the entire process with accurate timing and synchronization. The system's ability to reset and restart after completing tasks demonstrated its reliability and readiness for continuous operation.

The system achieved its objective of automating ginger processing. It provided a streamlined and user-friendly solution that reduced manual labour and improved processing efficiency. The results confirmed that the system was capable of handling real-world operational demands and could serve as a practical tool for small- to medium-scale ginger processing applications.

RECOMMENDATIONS

A simple recommendation for the system is to incorporate sensors, such as proximity or load sensors, at the inlet and outlet points to further automate the door operations. This would eliminate the reliance on fixed timers for opening and closing the doors, ensuring that the system adjusts dynamically based on the actual flow of ginger. This enhancement would improve processing efficiency and reduce the risk of jams or delays.

REFERENCES

[1] Ajav, E. A., & Ogunlade, C. A. (2014). Physical properties of ginger (Zingiber officinale). Glob. J. Sci. Front. Res, 14, 1-18.

[2] Arocha, C. G., & Simonyan, K. J. (2019b). Development of a Motorized Ginger Rhizomes Peeling Machine. Nigerian Journal of Technology, 38(3), Article 3. https://doi.org/10.4314/njt.v38i3.32

[3] Gao, R., Ye, F., Lu, Z., Wang, J., Li Shen, X., & Zhao, G. (2018). A novel two-step ultrasound post-assisted lye peeling regime for tomatoes: Reducing pollution while improving product yield and quality. Ultrasonics Sonochemistry, 45, 267–278. https://doi.org/10.1016/j.ultsonch.2018.03.021

[4] Gavahian, M., & Sastry, S. K. (2020). Ohmic-assisted peeling of fruits: Understanding the mechanisms involved, effective parameters, and prospective applications in the food industry. Trends in Food Science & Technology, 106, 345–354. https://doi.org/10.1016/j.tifs.2020.10.027

[5] Kate, A. E., & Sutar, P. P. (2018). Development and optimization of novel infrared dry peeling method for ginger (Zingiber officinale Roscoe) rhizome. Innovative Food Science & Emerging Technologies, 48,111–121. https://www.sciencedirect.com/science/article/pii/S1466856417304265

[6] Lavelli Vera, Carlo Pompei, Casadei Maria Aurelia. (2009). Quality of nectarine and peach nectars as affected by lye-peeling and storage. https://doi.org/10.1016/j.foodchem.2009.01.047

[7] Kumar G V, P., Khobragade, C. B., Gupta, R., & Raza, K. (2019). Development and Performance Evaluation of an Electric Motor Powered Ginger Washing-Cum-Peeling Machine. International Journal of Current Microbiology and Applied Sciences, 8, 722–737. https://doi.org/10.20546/ijcmas.2019.802.084

[8] Lalthantluangi, C. (2022). Production and Marketing of Ginger and Chillies in Champhai District, Mizoram (Doctoral dissertation, Mizoram University).

[9] Malhotra, V. (2024). Advanced Manufacturing Processes. CRC Press.

[10] Michael F. Ashby, 2004. Hugh Shercliff, David Cebon Introduction to Materials Science and Engineering: A Design Led Approach.

[11] Shen, Y.; Khir, R.; Wood, D.; Mchugh, T. H.; Pan, Z. Pear Peeling Using Infrared Radiation Heating Technology. Innov. Food Sci. Emerg. Technol. 2020, 65, 102474. DOI: 10.1016/j.ifset.2020.102474.

[12] Shinde, I. N., Babar, K. P., & Bornare, D. T. (2018). Development of peeling machine for ginger, potato and sweet potato. https://www.cabidigitallibrary.org/doi/full/10.5555/20193025067

[13] Prasanna Kumar, G.V., C.B. Khobragade, Rakesh Kumar Gupta and Kamran Raza. 2019. Development and Performance Evaluation of an Electric Motor Powered Ginger Washing-Cum-Peeling Machine. Int.J.Curr.Microbiol.App.Sci. 8(02): 722-737. doi: https://doi.org/10.20546/ijcmas.2019.802.084Preparation, pungency and bioactivity of gingerols from ginger (Zingiber officinale Roscoe).

[14] Michael F. Ashby, (2004). Hugh Shercliff, David Cebon Introduction to Materials Science and Engineering: A Design Led Approach.

[15] Ugoamadi, C. C. (2012). Development of a cassava pelleting machine. Nigerian Journal of Technology, 31(3), 233-240.

[16] Van Colenberghe, M. (2023). Manufacturing process automation by means of PLCs (Bachelor's thesis, Universitat Politècnica de Catalunya).

[17] Vidyarthi, S. K., El-Mashad, H. M., Khir, R., Zhang, R., McHugh, T. H., & Pan, Z. (2019). Tomato peeling performance under pilot scale catalytic infrared heating. Journal of Food Engineering, 246, 224–231. https://doi.org/10.1016/j.jfoodeng.2018.11.002